PONTIFICIA UNIVERSIDAD CATÓLICA DEL PERÚ

ESCUELA DE POSGRADO

Influencia de la temperatura del aire al interior del molde sobre las propiedades de los materiales compuestos de polietileno reciclado y madera capirona recuperada fabricados por moldeo rotacional

Trabajo de investigación para obtener el grado académico de

Maestro en Ingeniería y Ciencia de los Materiales

que presenta:

Ademir Alejandro Vilcayauri Rios

Asesor:

Julio Arnaldo Acosta Sullcahuamán

Lima, 2024

INFORME DE SIMILITUD

Yo, Julio Arnaldo Acosta Sullcahuamán, docente de la Escuela de Posgrado de la Pontificia Universidad Católica del Perú, asesor del trabajo de investigación titulado “Influencia de la temperatura del aire al interior del molde sobre las propiedades de los materiales compuestos de polietileno reciclado y madera capirona recuperada fabricados por moldeo rotacional”, del autor Ademir Alejandro Vilcayauri Rios, dejo constancia de lo siguiente:

- El mencionado documento tiene un índice de similitud de 13%. Así lo consigna el reporte de similitud emitido por el software *Turnitin* el 19 de febrero de 2024.
- He revisado con detalle dicho reporte y la Tesis o Trabajo de investigación, y no se advierte indicios de plagio.
- Las citas a otros autores y sus respectivas referencias cumplen con las pautas académicas.

Lugar y fecha: San Miguel, 08 de abril de 2024.

Apellidos y nombres del asesor / de la asesora: Acosta Sullcahuamán, Julio Arnaldo	
DNI: 07960574	Firma 
ORCID: https://orcid.org/0000-0002-1518-4282	

RESUMEN

En el procesamiento de compuestos de madera-plástico (*WPC*) mediante moldeo rotacional, puede ocurrir la descomposición térmica de la madera debido a las altas temperaturas del proceso. Sin embargo, puede evitarse controlando el pico de temperatura interna del aire (*PIAT*, por sus siglas en inglés). En esta perspectiva, el principal propósito de este trabajo es determinar cómo están relacionados el *PIAT* y las propiedades del *WPC* rotomoldeado entre sí. Para lograr esto, se procesaron varios materiales utilizando diferentes temperaturas de horno y tiempos de calentamiento. Como consecuencia, el *PIAT* alcanzó un valor específico durante el proceso en cada caso. Luego, se realizaron ensayos de caracterización para determinar las propiedades mecánicas y físicas de los materiales obtenidos. Finalmente, utilizando los resultados de las pruebas, se definió una relación entre el *PIAT* y esas propiedades. Los *WPC* rotomoldeados estaban compuestos por un 85% de polietileno de alta densidad reciclado (*HDPER*) y un 15% de partículas de madera de capirona (*CWP*), pero también se procesaron materiales compuestos por un 100% de *HDPER*. Los resultados muestran que se requiere un *PIAT* de 208 °C para que un *WPC* rotomoldeado se densifique completamente. Bajo esta condición, tiene propiedades óptimas y no sufre degradación térmica. En cuanto al material compuesto por un 100% de *HDPER*, se necesita un *PIAT* de 233 °C para alcanzar dicho estado. Además, utilizando la segunda derivada de los perfiles de temperatura interna del aire, también se identificaron el comienzo y el final de las seis fases del proceso de moldeo rotacional.

ABSTRACT

In the processing of wood-plastic composites (*WPC*) by rotational molding, thermal decomposition of wood can occur due to the high temperatures of the process. However, it can be avoided by controlling the peak internal air temperature (*PIAT*). In this perspective, the main purpose of this work is to determine how the *PIAT* and the properties of the rotomolded *WPC* are related to each other. To achieve this, several materials were processed using different oven temperatures and heating times. As a consequence, the *PIAT* reached a specific value during the process in each case. Then, characterization tests were carried out to determine mechanical and physical proprieties of the obtained materials. Finally, using the test results, a relationship between the *PIAT* and those properties was defined. The rotomolded *WPC* were made of 85% of recycled high-density polyethylene (*HDPER*) and 15% of capirona wood particles (*CWP*), but materials made of 100% of *HDPER* were also processed. Results show that a *PIAT* of 208 °C is required for a rotomolded *WPC* to be fully densified. Under this condition, it has optimal properties and it does not undergo thermal degradation. As for the material made of 100% of *HDPER*, a *PIAT* of 233 °C is necessary to reach such state. In addition, using the second derivative of the internal air temperature profiles, the beginning and end of the six phases of the rotational molding process were identified, too.

TABLA DE CONTENIDO

1. INTRODUCTION 2
2. MATERIAL AND METHODS 3
2.1. Materials 3
2.1.1. Recycled high-density polyethylene (HDPER) 3
2.1.2. Capirona wood particles (CWP) 3
2.1.3. Composite powder (HDPER-CWP powder) 4
2.2. Equipment 4
2.2.1. Rotational molding machine 4
2.2.2. Molds 4
2.2.3. Temperature measurement system 5
2.3. Rotational molding parameters 5
2.4. Experimental procedure 6
2.5. Characterization tests 6
2.5.1. Morphology 6
2.5.2. Tensile test 7
2.5.3. Density and porosity 7
2.5.4. Water absorption 7
2.5.5. Melt flow index (MFI) 7
2.5.6. Fourier transform infrared spectroscopy (FTIR) 7
2.5.7. Scanning electron microscopy (SEM) 8
3. RESULTS AND DISCUSSION 8
3.1. Analysis of temperature/time profiles 8
3.2. Influence of *CWP* on the *IAT* profiles of rotomolded materials 10
3.3. Influence of T_H on the *IAT* profiles of rotomolded *WPC* 11
3.4. Influence of t_H on the *IAT* profiles of rotomolded materials 12
3.5. Results of characterization tests 13
3.5.1. Differential scanning calorimetry (DSC) and MFI 13
3.5.2. Morphology 14
3.5.3. Influence of the PIAT on mechanical properties 15
3.5.4. Influence of the PIAT on physical properties 18
3.5.5. FTIR 20
3.5.6. SEM 20
4. CONCLUSIONS 22
References 24

TABLA DE FIGURAS

Fig. 1. Temperature measurement system. 5
Fig. 2. Samples of rotomolded *WPC* 6
Fig. 3. Temperature/time profiles of a rotomolded *WPC* (T_H of 300°C, t_H of 26 min). 8
Fig. 4. Influence of *CWP* and T_H on the *IAT* profiles 11
Fig. 5. Set of *IAT* profiles and their 2nd derivatives. 13
Fig. 6. Morphology of the rotomolded *WPC* from Group B: 15
Fig. 7. Mechanical properties of the rotomolded materials from Groups A and B. 16
Fig. 8. Physical properties of the rotomolded materials. 18
Fig. 9. Actual thickness of the rotomolded materials from Group B. 21
Fig. 10. *FTIR* spectra of the rotomolded materials from Group A. 21
Fig. 11. Facture surface of a tensile test specimen 22

INFLUENCE OF THE PEAK INTERNAL AIR TEMPERATURE ON THE PROPERTIES OF WOOD-PLASTIC COMPOSITES MADE OF RECYCLED POLYETHYLENE AND CAPIRONA WOOD PARTICLES PROCESSED BY ROTATIONAL MOLDING

Ademir Vilcayauri-Rios[1], Adan Arribasplata-Seguin[1,2], Roger Quispe-Dominguez[3], Julio Acosta-Sullcahuamán[1,2]

[1]Escuela de Posgrado, Programa de Maestría en Ingeniería y Ciencia de los Materiales, Sección Ingeniería Mecánica, Pontificia Universidad Católica del Perú, Av. Universitaria 1801, Lima 32, Perú.

[2]Escuela de Posgrado, Programa de Doctorado en Ingeniería, Sección Ingeniería Mecánica, Pontificia Universidad Católica del Perú, Av. Universitaria 1801, Lima 32, Perú.

[3]Escuela de Profesional de Ingeniería Mecánica, Universidad Nacional de San Antonio Abad del Cusco, Av. De La Cultura 773, Cusco 08003, Perú.

Corresponding author: adan.arribasplata@pucp.edu.pe
E-mail addresses: vilcayauri.ademir@pucp.edu.pe, (A. Vilcayauri-Rios), adan.arribasplata@pucp.edu.pe (A. Arribasplata-Seguin), roger.quisped@unsaac.edu.pe (R. Quispe-Dominguez), jacosta@pucp.edu.pe (J. Acosta-Sullcahuamán).

ABSTRACT

In the processing of wood-plastic composites (*WPC*) by rotational molding, thermal decomposition of wood can occur due to the high temperatures of the process. However, it can be avoided by controlling the peak internal air temperature (*PIAT*). In this perspective, the main purpose of this work is to determine how the *PIAT* and the properties of the rotomolded *WPC* are related to each other. To achieve this, several materials were processed using different oven temperatures and heating times. As a consequence, the *PIAT* reached a specific value during the process in each case. Then, characterization tests were carried out to determine mechanical and physical proprieties of the obtained materials. Finally, using the test results, a relationship between the *PIAT* and those properties was defined. The rotomolded *WPC* were made of 85% of recycled high-density polyethylene (*HDPER*) and 15% of capirona wood particles (*CWP*), but materials made of 100% of *HDPER* were also processed. Results show that a *PIAT* of 208 °C is required for a rotomolded *WPC* to be fully densified. Under this condition, it has optimal proprieties and it does not undergo thermal degradation. As for the material made of 100% of *HDPER*, a *PIAT* of 233 °C is necessary to reach such state. In addition, using the second derivative of the internal air temperature profiles, the beginning and end of the six phases of the rotational molding process were identified, too.

Highlights:

- *HDPER* and *CWP* recovered from scrap wood were used for making rotomolded *WPC*.
- Internal air temperature profiles of rotomolded *WPC* were registered.
- Critical temperatures for the processing of rotomolded *WPC* were identified.
- The influence of the *CWP* on the sintering of *HDPER* powder was assessed.
- A relationship between the *PIAT* and the properties of rotomolded *WPC* was found.

Key words: rotational molding, sintering, densification, wood-plastic composites, recycled polyethylene, natural fibers, wood particles, internal air temperature profile, peak internal air temperature.

1. INTRODUCTION

The rotational molding process is used for the manufacturing of hollow parts from a plastic material in the form of powder or viscous liquid [1]. By using this process, it is possible to obtain large-volume or complex-shaped objects made of a single piece without residual stress at low cost [2]. The process takes places in four cycles: (i) charging the material, (ii) heating the mold, (iii) cooling the mold, and (iv) demolding the rotomolded part.

The interest for using natural fibers to make polymer composites by rotational molding has grown remarkably in the last years because of their many advantages [3]. Natural fibers have low density, high specific strength and modulus. Besides, these fibers are low-cost, nonabrasive, hydrophilic and biodegradables. Because of its intrinsic characteristics, this type of fibers can be employed as alternative and ecologic reinforcement. However, these fibers are incompatible with most polymers, which is a disadvantage that seriously limits their use.

Despite that fact, several attempts have made for making natural fibers composites by rotational molding. In most cases, polyethylene (*PE*) has been the most commonly used matrix [3]. On the contrary, several fibers have been employed to see if they can be incorporated within the rotational molding process or not. Some of them are sisal [4-5], flax [6-8], agave [9-12], pine wood [11], coir [11-12], bamboo [13], and hemp [8]. Natural fibers in the form of flour like rice shell [4], pecan shell [4], wheat bran [14], buckwheat husk [15], coir [16], maple wood [17-20], capirona wood [21], and pine wood [21-22] have been used as well.

From all the material mentioned above, the wood-plastic composites (*WPC*) deserve special attention. These materials are made of wood (in the form of fibers, particles or flour) and a thermoplastic or a thermoset. Basically, the *WPC* can be divided into two groups [23]. In the first group, the wood elements can work as a reinforcement or filler. Thus, the quantity of wood elements is much less than the matrix. In the second group (known also as wood-based composites), the matrix works as a binder, so the quantity of wood elements is much higher than the matrix. In contrast to wood, the *WPC* from the first group present some advantages [24]: (i) they have good thermal stability in wet and dry environments, (ii) no treatment or paint is required to protect their surface, (iii) they are resistant to termites and fungi, (iv) complex shapes can be made without machining, and (v) they are more environmental-friendly than wood treated with preservatives. Nevertheless, wood has an important disadvantage to be considered. Like any other natural fiber, it has low thermal resistance and its thermal decomposition begins approximately at 200 °C [25]. In despite of its limitations, wood is used as raw material for making *WPC* commercial products [24].

In the case of rotomolded *WPC,* studies have demonstrated that these materials have a remarkable aesthetic appearance since the wood particles are evenly distributed all over the matrix [21-22]. However, their mechanical properties and water absorption are negatively affected by the presence of such particles. In general, lignocellulosic fibers contain polar hydroxyl groups on their surface [26]. Because of these groups, natural fibers are not compatible with the non-polar thermoplastics such as PE, so adhesion between both materials is poor, and it causes mechanical weakening [27-28]. It is possible to improve the adhesion by treating the fibers with coupling agents such as silane [7] and anhydride grafted polyethylene

(*MAPE*) [12, 18-20, 29]. By doing this, natural fibers are no longer as green and ecological as before the treatment.

The measurement of internal air temperature (*IAT*) can be a powerful tool to study natural fibers polymer composites made by rotational molding, but it has been used in very few investigations related to this topic. From this measurement, an *IAT* profile (*IAT* versus time) is obtained. This profile depends on the design of the rotational molding machine, the characteristics of the plastic material, the shape of the product to be molded, and the characteristics of mold. Therefore, there is a particular *IAT* profile for every equipment-material-form system. As there are many variables involved, this profile is normally determined by experimentation. The information derived from an *IAT* profile is very relevant for the rotational molding process. According to Nugent [30], the critical points of this process can be identified by using an *IAT* profile: (i) beginning and end of the powder adhesion to the mold surface, (ii) *PIAT*, (iii) beginning and end of crystallization in the case of semicrystalline thermoplastics, and (iv) demolding point for solidified part. One of the most important points within a certain *IAT* profile is the *PIAT.* It is known that this temperature must reach a specific value to achieve the fully densification of the plastic layer formed against the inner mold surface. In this context, the main objective of this work is to determine how the *PIAT* influences on the mechanical and physical properties of *WPC* made of recycled *HDPER* and *CWP* that are processed by rotational molding. This work is a continuation of a previous research [21]. Thus, the results found in that work will be used as the basis for the development of present study.

2. MATERIAL AND METHODS

2.1. Materials

2.1.1. Recycled high-density polyethylene (HDPER)

A *HDPER* powder was required for making the rotomolded *WPC* of this investigation. The *HDPER* came from unused white bottle caps, which were supplied by ALUSUD PERU S.A. These caps were made by injection molding of BorPureTM MB6562, which is a commercial virgin high density polyethylene (*HDPE*). In order to get a suitable *HDPER* powder for rotational molding process, the caps were cut and pulverized to reach an average particle size of 500 µm (35 mesh). Notice that the plastic coming from the bottle caps is called injected *HDPE* in this work. This material has a density of 0,955 g/cm^3 (ASTM D792), and its melt flow index is 1,8 g/10 min when a temperature of 190 °C and a weight of 2,16 kg are used (ASTM D1238). In addition, results from a previous investigation [21] show that thermal degradation of *HDPE* starts at 290 °C and the highest mass loss rate occurs at 470 °C. These results are consistent with other studies [31-32].

2.1.2. Capirona wood particles (CWP)

The wood particles came from *calycophyllum spruceanum* or capirona tree. It is indigenous to the Amazon rainforest, so it grows in the South American countries of Bolivia, Colombia, Brazil, Ecuador, and Peru. The *CWP* were recovered from furniture factories located on Villa El Salvador, Lima, Perú. Note that these particles came from homogenous scrap wood (sawdust and woodchips) which is generated during furniture manufacturing. These particles were sieved to obtain particles of 500 µm. Since the size is smaller than 850 µm, the *CWP* can be considered as wood flour [33]. In a previous work [21], it was

demonstrated that this particle size is appropriate for making *WPC* by rotational molding. In this study, the *CWP* were not treated with any kind of coupling agent to keep their natural and ecological feature either. Besides, under supply conditions, the capirona wood has a moisture content of 14% and its dry density is 0,737 g/cm^3 (ASTM D2395). As it has been proved that wood moisture is removed before the sintering begins [34], it was not required to dry the *CWP*. For this reason, dry density was used for the calculation of the quantity of *CWP* that is required for making a rotomolded *WPC* sample. On the other hand, in a previous study [21], it has also been determined that thermal decomposition of capirona wood begins at 200 °C.

2.1.3. Composite powder (HDPER-CWP powder)

In this study, *HDPER* powder and *CWP* were dry-blended to obtain the composite powder that was used as raw material for the rotational molding process. In this case, 85% of *HDPER* and 15% of *CWP* (volume fractions) were employed for elaborating this powder. Then, as a *WPC* cylindrical sample has a nominal volume of 895 cm^3 (nominal thickness of 5 mm), 727 g of *HDPER* and 101 g of *CWP* (828 g of composite powder) were required for making each sample. Additionally, 855 g of *HDPER* powder was necessary for making a sample of the same volume that does not contain *CWP*. Rule of mixtures was employed for mass calculation in both cases.

2.2. Equipment

2.2.1. Rotational molding machine

A shuttle-type rotational molding machine was used in this investigation. It was designed by our research team and fabricated with funds from the Peruvian government. This machine has a straight arm whose rotation speeds can be set between 4 and 50 RPM at any of the two rotation axes. It also has an electric oven of 22 kW that works with a centrifugal fan of 1200 CFM for heating and it can reach a maximum temperature of 350 °C. For cooling, it has a couple of axial fans whose speeds can be regulated from 0 to 6800 CFM.

2.2.2. Molds

Two stainless steel cylindrical molds were used for making the rotomolded samples. Each mold has a thickness of 1/8" and the dimensions of its cavity are Ø215 mm (top face) x Ø200 mm (bottom face) x 185 mm (height). A draft angle of 2° was considered, too. One of the molds was modified in order to measure 03 important temperatures during the rotational molding process: (i) mold outer surface temperature (T_{OS}), (iii) mold inner surface temperature (T_{IS}) and (iii) internal air temperature (*IAT*). Type K thermocouples were employed for measuring each of these temperatures. Different accessories were specially designed for fixing those thermocouples to the mold. Fig. 1 shows how these instruments were placed in the mold. First, the tip of the T_{OS} thermocouple was positioned in the middle of the outer surface of the mold. Second, the tip of the T_{IS} thermocouple was located in the middle of the outer surface of the cylindrical samples, so it was able to measure the temperature of the rotomolded materials. Third, the tip of the *IAT* thermocouple was placed in the middle of the mold cavity. Notice that a tube of polytetrafluorethylene with a hole of 1/2 in was used for venting as well.

2.2.3. Temperature measurement system

Using the temperature measurement system shown in Fig. 1, it was possible to record the three temperatures described previously. Its main components are: (i) three type K thermocouples, (ii) a three-channel temperature datalogger EXTECH SD200, and (iii) a thermal protection box. The system was located on the straight arm of the molding machine to rotate simultaneously with the mold during the whole process. In order to keep the temperature datalogger safe from the heat of the oven, it was imperative to place it inside the thermal protection. The system is not prepared for showing the temperature/time profiles during the execution of the rotational molding process. Then, it was necessary to download the data into a computer to plot and analyze these profiles at the end of the process. The datalogger registered the temperatures using a data sampling rate of 5 s and it recorded all data on a SD card. The system was also designed by our research team and fabricated with funds from the Peruvian government.

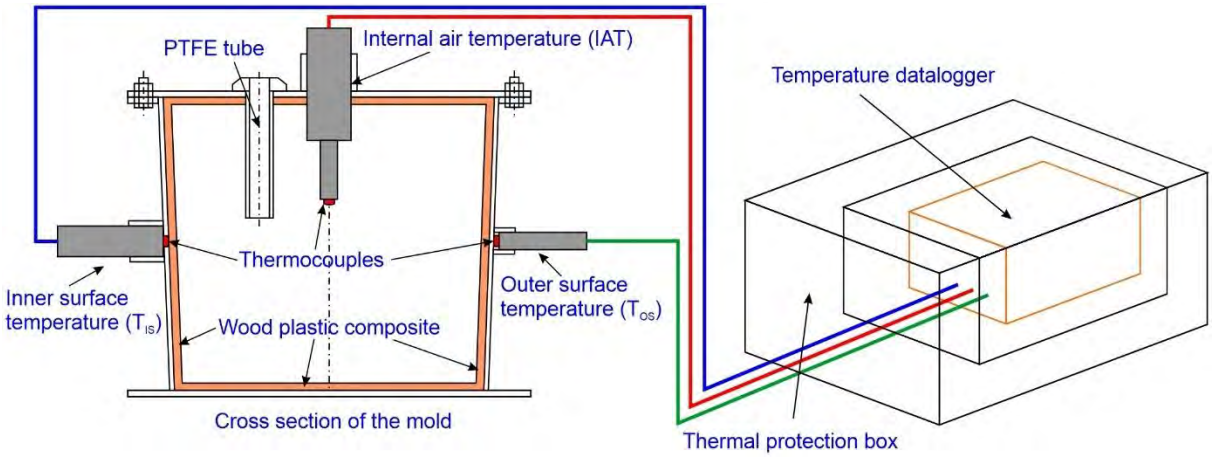

Fig. 1. Temperature measurement system.

2.3. Rotational molding parameters

All rotational molding parameters have a particular influence on the quality and the final properties of the rotomolded materials. Nevertheless, these were set to a specific value considering the main objective of this study, except for the oven temperature (T_H) and the heating time (t_H). In this case, different values for T_H and t_H were used in order to control the final value of the *PIAT*. For the rest of the parameters, recommended values were employed. For example, *PE* powder having a size distribution of 35 mesh is typically used as it offers the best compromise between grinding costs and the fusion characteristics of the plastic [35-36]. On the other hand, it has been demonstrated that a rotomolded *WPC* made of 85% of *HDPER* and 15% of *CWP* shows the best mechanical properties [21]. For that reason, those volume fractions were considered for elaborating the composite powder in this study. In the same way, a speed ratio of 4:1 was selected since it is commonly employed for making symmetrical products. Finally, regarding the cooling method, forced air was required due to the high crystallinity of the *HDPER*. In this case, a cooling time (t_C) of 30 min was necessary for the outer surface of the mold to reach a temperature of 40 °C when a cooling air flow of 4200 CFM is used.

2.4. Experimental procedure

It is clear that, for a certain machine-mold-material system, the T_H and the t_H must be selected carefully to reach the *PIAT* that is required for achieving the full densification of the material without causing its thermal degradation during the heating cycle. Consequently, different combinations of T_H and t_H were used for making the rotomolded materials shown in Table 1. For example, the materials from Group B are made of 85% of *HDPER* and 15% of *CWP*, and these were processed using a T_H of 260 °C and a certain t_H. As a result, seven different rotomolded materials were obtained. In each case, the *PIAT* reached a specific value during the process. As seen in Table 1, twenty-eight different materials were molded for this investigation. All of them were subjected to mechanical and physical characterization tests. Test results were used to find a relationship between the *PIAT* and the properties of the rotomolded materials. Some cylindrical samples of rotomolded *WPC* are shown in Fig. 2.

Table 1. Rotomolded materials.

Group	Material composition	T_H (°C)	t_H (min)							
A	100% *HDPER*	260	20	25	30	35	40	45	50	–
B	85% *HDPER* / 15% *CWP*	260	20	25	30	35	40	45	50	–
C		280	16	20	24	28	32	36	40	44
D		300	17	20	23	26	29	32	–	–

Fig. 2. Samples of rotomolded *WPC*.

2.5. Characterization tests

2.5.1. Morphology

In order to evaluate the sintering and densification of the rotomolded *WPC*, a Leica S6D stereoscope equipped with a Leica DFC320 camera was used to observe and photograph the inner surface of the cylindrical samples made by rotational molding. No prior surface preparation was required.

2.5.2. Tensile test

Two cylindrical samples were rotomolded for each of the 28 materials indicated in Table 1. From each sample, 04 tensile specimens (ASTM D638, type I) were obtained by using a CNC router machine. Tensile test was conducted using a Zwick/Roell Z050 machine equipped with a 50 kN load cell. A speed of testing of 5 mm/min was selected. For each material, 08 specimens were used to determine tensile strength (σ_M), elastic modulus (E_M) and tensile strain associated with tensile strength (ε_M).

2.5.3. Density and porosity

Density of rotomolded *WPC* was measured by volumetric displacement according to ASTM D792. This standard was also used to determine the density of the injected *HDPE* that comes from the recycled plastic caps. Similarly, moisture content and density of capirona wood was determined by volumetric displacement according to ASTM D2395. In this case, specimens were dried in an oven at 103 °C for 24 h to eliminate moisture and cooled in a desiccator.

On the other hand, porosity of a certain rotomolded material was estimated using the value of its density and Eq. 1 as follows:

$$P = (\rho_R - \rho) / \rho_R * 100\ \% \qquad \text{Eq. 1}$$

Where, P is the porosity, ρ_R is a reference density, and ρ is the density of the rotomolded material. For this particular case, the density of the injected *HDPE* (0,955 g/cm^3) was used as the ρ_R. Since injection molding was employed to make the recycled plastic caps, it is presumed that injected *HDPE* is free of pores. So, its density is suitable as a reference.

2.5.4. Water absorption

In order to determine water absorption of rotomolded materials, 08 specimens of 15 mm x 40 mm were used in each case. Specimens were dried in an oven at 50 °C for 24 h and cooled in a desiccator. Then, they were immediately weighed to determine its dry mass before being submerged into distilled water for 24 h. After that, specimens were removed from the water one at a time, wiped off with a dry cloth, and weighed to measure its wet mass. The increase in weight of each specimen, gained during water immersion, was calculated by subtracting specimen's wet and dry mass. Finally, water absorption is calculated by dividing this increase in weight by the dry mass.

2.5.5. Melt flow index (MFI)

MFI tests were conducted according to ASTM D1238 using a Zwick/Roell MFlow equipment. MFI tests were performed on: (i) virgin *HDPE* (Borealis BorPureTM MB6562), (ii) *HDPER* powder and (iii) a rotomolded material made of 100% *HDPER* (T_H of 260 °C and t_H of 40 min). In all cases, a temperature of 190 °C and a weight of 2,16 kg were employed.

2.5.6. Fourier transform infrared spectroscopy (FTIR)

In order to study thermal-oxidation of *HDPER*, *FTIR* spectra of rotomolded materials made of 100% of *HDPER* were obtained using a BRUKER TENSOR 27 IR.

2.5.7. Scanning electron microscopy (SEM)

The FEI QUANTA 650 FEG microscope was used to observe the fracture zone of tensile specimens. The samples were photographed using a large field detector at 15 kV and working distances of 10 mm. Specimens were not coated for this test.

3. RESULTS AND DISCUSSION

3.1. Analysis of temperature/time profiles

As an example, Fig. 3 shows the set of temperature/time profiles of a rotomolded *WPC* from Group D. It was molded with a T_H of 300 °C (horizontal black line) and a t_H of 26 min (see Table 1). In this case, the purple, light blue and green curves correspond to T_{OS}, T_{IS}, and *IAT profiles*, respectively. Similarly, the blue and red curves are the first and second derivative with respect to time of the *IAT* profile. While the first derivative corresponds to the instantaneous heating rate (positive value) or cooling rate (negative value) of the air inside the mold, the second derivative measures how this rate varies, so its local maximums and minimums correspond to the inflection points of the *IAT* profile.

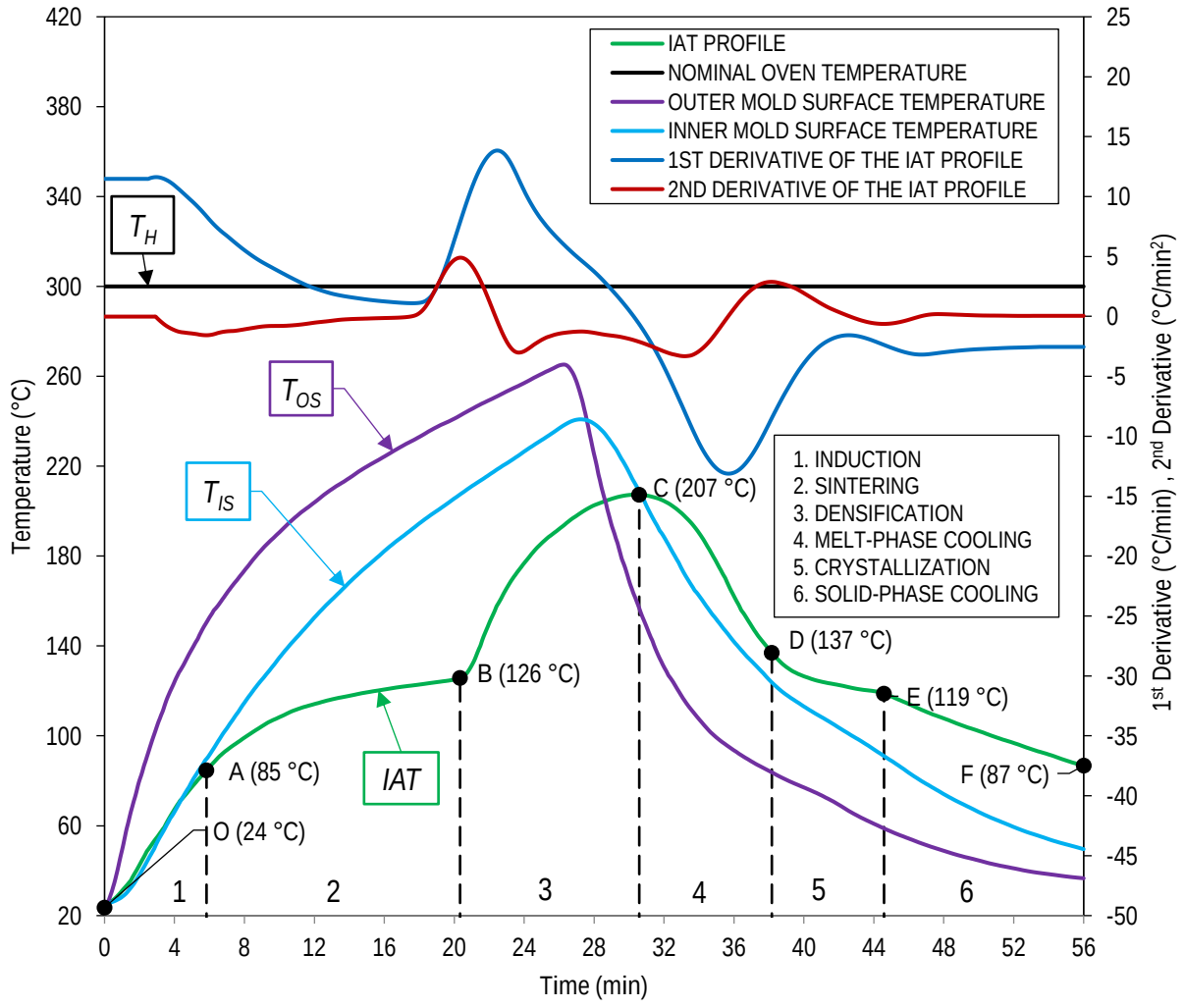

Fig. 3. Temperature/time profiles of a rotomolded *WPC* (T_H of 300°C, t_H of 26 min).

Taking into account the idea presented by González-Núñez et al. [37], second derivative was used to identify the inflection points (critical points): *A*, *B*, *C*, *D* and *E* of the *IAT* profile shown in Fig. 3. The critical

points are extremely important for the rotational molding process. These define the beginning and end of the six phases that take place during the transformation of the composite powder into a solid monolithic wood-plastic layer against the inner mold surface. Notice that dashed vertical lines were drawn to highlight those points.

From the previous calculation, the beginning and end of those phases has been identified: (i) induction (OA), (ii) sintering (AB), (iii) densification (BC), (iv) melt-phase cooling (CD), (v) crystallization (DE), and (vi) solid-phase cooling (EF) [30]. It is observed that the *IAT* profile of this rotomolded *WPC* exhibits a behavior which is typical of a thermoplastic. It was expected since this material is mostly constituted by *HDPER*. So, as a general result, when the quantity of *CWP* is less than or equal to 15%, it can be affirmed that the presence of *CWP* does not affect the shape of the *IAT* profile.

During the induction (OA), the composite powder starts to heat up, but it does not undergo any physical change while the mold rotates biaxially inside the oven. Then, when certain portion of the powder and the mold inner surface are hot enough, the *HDPER* particles stick to that surface and to each other, which indicates the beginning of the sintering (AB). At the very beginning of this phase, a thin layer of composite material is formed all over the mold cavity. As the *IAT* increases, successive layers are incorporated one over another until all the powder is consumed. As a consequence of particle coalescence, a highly porous single layer of composite material is obtained at the end of this phase. It can be noticed that the *CWP* are uniformly distributed all over the layer and these are no able to move freely due to the viscoelasticity of the matrix. In the sintering, the instantaneous heating rate increases slowly because the composite powder needs to absorb heat to soften and melt. In this particular case, according to the second derivative, the sintering begins and ends when the *IAT* is 85 °C and 126 °C, respectively.

Once all the composite powder is fully adhered to the mold cavity, the densification (BC) takes place. During this phase, the traces of the air trapped within the layer of composite material gradually transform into air bubbles as the temperature increases. These bubbles disappear through dissolution and diffusion mechanisms [38]. In addition, *HDPER* behaves like a high-viscosity fluid. As a result, first derivative shows that heat transfer improves because the air inside the mold heats up faster, despite the presence of the *CWP*. In this case, the *PIAT* reached 207 °C, but this value can be controlled by regulating the value of t_H, which defines the end of the heating cycle. Note that it takes 4,6 min for the machine-mold-material system to reach this *PIAT* after the heating cycle ends because of thermal inversion.

In the melt-phase cooling (CD), the layer of composite material simply cools down because no physical change is appreciated. It is observed that the *IAT* and T_{IS} profiles almost decrease at the same cooling rate during this phase. However, that changes drastically as crystallization (DE) occurs. This process is exothermic, so the air inside the mold absorbs the energy released by layer of composite material. Thus, the air cools down more slowly. For this particular case, it has been determined that the crystallization begins and ends when the *IAT* is 137 °C and 119 °C, respectively. Finally, the last part of the cooling cycle corresponds to the final solid-phase cooling (EF). During this phase, the rotomolded *WPC* shrinks, facilitating the extraction of the cylindrical sample.

Concerning the time spent on each phase, it can be noticed that the duration of the induction is the shortest of all (5,8 min), but it still represents 10% of the time spent for the whole rotational molding process (process time = t_H + t_C = 26 min + 30 min = 56 min). In contrast, the duration of the sintering is the longest of all (14,5 min). Certainly, 26% (one-fourth) of the process time has been required to develop this phase. In relation to t_H, the duration of the sintering represents 56% of that time. This means that more than half of the time spent for heating cycle has been used for the sintering.

In the same way, the duration of the densification (10,3 min) is also significant as it represents 18% of the process time. According to Gogos [39], 40% of the time for the rotational molding process is required to eliminate air bubbles during the densification. Notice that the end of this phase is regulated by the *PIAT* to be achieved. So, it is likely that the heating time used by Gogos was very high in order to eliminate the air bubbles completely.

In the cooling cycle, the durations of melt-phase cooling (7,6 min) and the solid-phase cooling (11,4 min) represent 14% and 20% of the process time, respectively. This means that 34% (one-third) of the process time was spent on these two phases. Finally, the duration of the crystallization is 6,4 min and it corresponds to 12% of the process time.

Regarding the T_{OS} profile, it has a maximum value of 265 °C at the end of the heating cycle and a value of 37 °C at the end of the cooling cycle. As for T_{IS} profile, it is observed that it lags behind T_{OS} profile due to the thermal resistance of the mold as expected.

On the other hand, the maximum temperature of the T_{IS} profile has been called the peak inner surface temperature (PT_{IS}). Considering how the T_{IS} was measured, the PT_{IS} is the highest temperature that a rotomolded material reached during its processing. The PT_{IS} can be used as a reference for thermal degradation and, in this particular case, it is 241 °C.

3.2. Influence of *CWP* on the *IAT* profiles of rotomolded materials

Fig. 4(a) shows the *IAT* profile of two different materials. One of them is made of 100% *HDPER* (blue curve), and the other one is made of 85% *HDPER* and 15% *CWP* (green curve). These materials were processed using the same conditions as indicated in Section 2.3. Particularly, a T_H of 260 °C and t_H of 30 min were employed in this case.

Notice that *IAT* profiles exhibit the same behavior during the induction, revealing that the presence of *CWP* has no influence on this phase. However, the duration of the sintering is 3,0 min longer in the case of material that contains *CWP*. This means that a composite powder requires a longer time to fully adhere to the mold cavity during the sintering. Clearly, the presence of *CWP* has a negative effect as it extends the duration of the sintering and delays plastic particle coalescence. Previously, this phenomenon has been studied under static conditions [40] and under dynamic o real conditions [21]. Nonetheless, these results are mainly qualitative and cannot be directly applied to the rotational molding process. By using the *IAT* profiles and their second derivatives, it has been possible to measure accurately the negative effect of *CWP* during the sintering in this case.

Capirona wood can be considered as a hardwood due to its density. Therefore, its thermal conductivity is approximately 0,16 W/mK [41], which is three times lower than that of *HDPE* (0,51 W/mK [42]). From this, it can be inferred that the thermal insulation behavior of capirona wood is responsible for the increase in the duration of the sintering. In spite of this fact, the sintering for both materials ends when the *IAT* is 126 °C. This proves that presence of *CWP* does not affect the *IAT* that defines the end of the sintering.

During the densification, the *IAT* profiles present similar trends as well as their first derivatives, but they are out of synchronization since the time spent for the sintering is different in each case. This demonstrates that the air inside the mold heats at the same rate during the densification whether the material contains *CWP* or not. In despite of the thermal insulation behavior of the *CWP*, it is evident these particles have no influence on the heat transfer in this phase. Furthermore, it can be observed that the *PIAT* of both materials is different, which means that the level of densification is also different in each case.

Finally, heat transfer is not affected by presence of *CWP* during the cooling cycle because the *IAT* profiles exhibit the same behavior. For both of them, it has been determined that the beginning and end of the crystallization occur when the *IAT* is 132 °C and 120 °C, respectively.

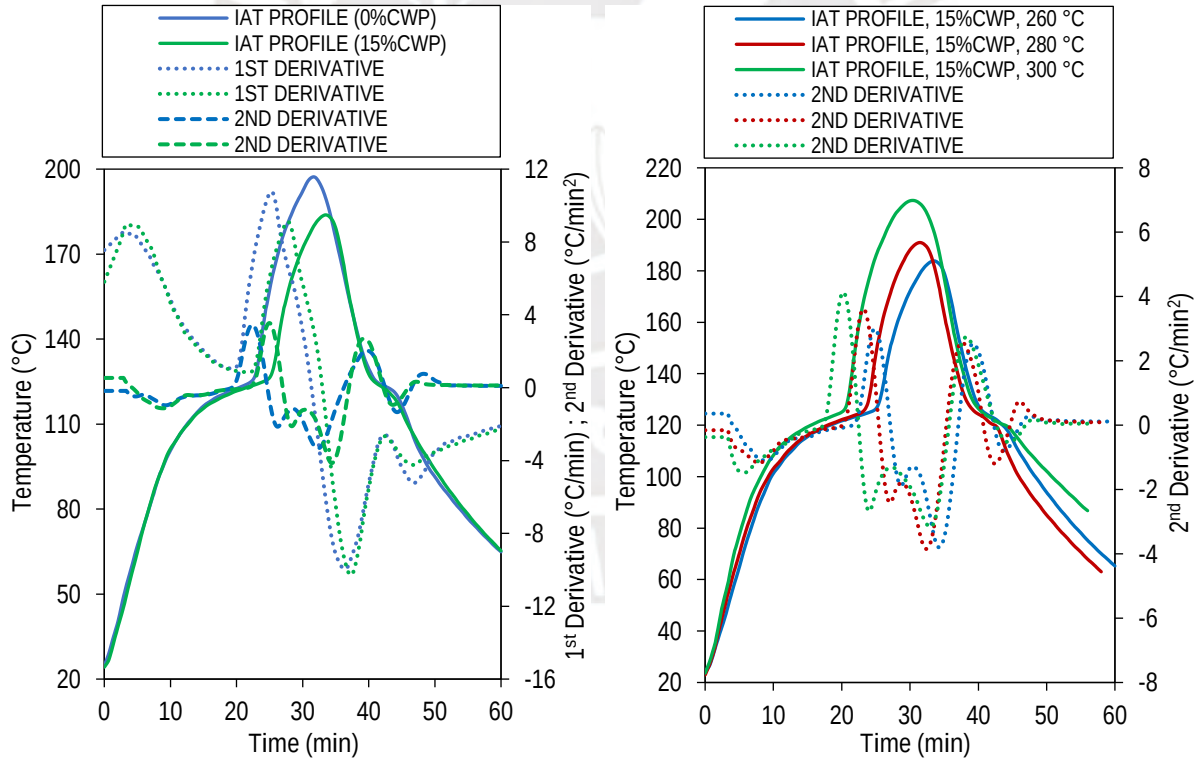

(a) Influence of *CWP*. (b) Influence of T_H

Fig. 4. Influence of *CWP* and T_H on the *IAT* profiles

3.3. Influence of T_H on the *IAT* profiles of rotomolded *WPC*

Fig. 4(b) shows the *IAT* profile of 03 rotomolded *WPC* made of 85% *HDPER* and 15% *CWP*. These were molded with different T_H and t_H: (i) 260°C - 30 min, (ii) 280 °C - 28 min, (iii) 300 °C - 26 min. The rest of the molding parameters were set as indicated in Section 2.3.

First, these results show that the *IAT* that settles the end of the induction depends on the T_H employed as this varies between 85 °C and 93 °C. Then, the duration of sintering also varies with the T_H and it is 16,5 min for 260 °C, 15,4 min for 280 °C and 14,5 min for 300 °C. Certainly, the duration of this phase gets shorter as T_H increases. In addition, it is observed that the end of the sintering takes place once the *IAT* is 126 °C in all cases. Therefore, the *IAT* that settles the end of this phase is independent of the T_H employed. Finally, it can be inferred from Fig. 4(b) that the t_H required for reaching a certain *PIAT* can be short provided that a high T_H is used. For example, the *PIAT* of the material molded with a T_H of 300 °C is the highest, in spite of the fact that the t_H is the shortest. It is clear that a T_H of 300 °C presents more advantages.

Concerning the cooling cycle, results show that the *IAT* which settle the beginning and end of the crystallization are also independent of the T_H. It has been determined that this phase begins and ends when the *IAT* is 135 °C and 120 °C, respectively.

3.4. Influence of t_H on the *IAT* profiles of rotomolded materials

Fig. 5 presents the *IAT* profiles of the rotomolded materials from the Groups A (0% *CWP*) and B (15% *CWP*). According to Table 1, these were molded with a T_H of 260 °C and different t_H. Using the second derivative, it was possible to identify the critical points: *A*, *B*, *C*, *D*, and *E* (shown in Fig. 3) and their corresponding temperatures for all *IAT* profiles. For each critical point, all the obtained temperatures were averaged to have a representative value. Notice that the *IAT* profiles of the materials from Groups C and D were also registered, so they were also included in this analysis.

Results indicate that sintering begins when the *IAT* is between 85 and 95 °C (point A), and it ends when the *IAT* is 126 ± 0,6 °C (point B). Notice that this particular temperature only depends of the *HDPER* characteristics, and rotational molding parameters do not have any effect on it. In the same way, the *IAT* that settles the beginning and end of the crystallization is 133 ± 3,2 °C (point D) and 119 ± 1,3 °C (point E), respectively.

Zepeda-Rodríguez et al. [43] has reported an *IAT* profile for a linear medium-density polyethylene (*LMDPE*). In that case, they indicated that sintering begins and ends when the *IAT* is 69 °C and 131 °C, respectively and crystallization begins and ends when the *IAT* is 118 °C and 88 °C, respectively. The *LMDPE* (128 °C [43]) and the *HDPER* (133 °C, see Section 3.5) have similar melting temperatures. It may be the reason why the *IAT* associated with the end of the sintering are similar, too. In contrast, the crystallinity of both materials is completely different: (i) 43% for *LMDPE* [43] and 71% for *HDPER* (see Section 3.5). Then, it is reasonable that the *IAT* associated with the crystallization are different as well.

Regarding the temperature that determines the end of the densification (point C or *PIAT*), Fig. 4 shows clearly that it depends on the value set for the t_H, in contrast to the temperatures indicated above. Similarly, it is evident that the PT_{IS} of every T_{SI} profile depends on the t_H, too. In the case of Groups A and B, the PT_{IS} were practically the same because these were processed with the same T_H and t_H. The PT_{IS} of Group A were: 173 °C (20 min), 191 °C (25 min), 205 °C (30 min), 218 °C (35 min), 230 °C (40 min), 238 °C

(45 min) and 245 °C (50 min). The PT_{IS} of Group B were: 176 °C (20 min), 193 °C (25 min), 209 °C (30 min), 222 °C (35 min), 233 °C (40 min), 239 °C (45 min) and 247 °C (50 min).

It is important to note that the presented results are valid when the quantity of *CWP* is less than or equal to 15%. So, it presumed that some of the critical points may vary if the quantity of *CWP* is higher. Further investigation must be carried out to see what happens in that situation.

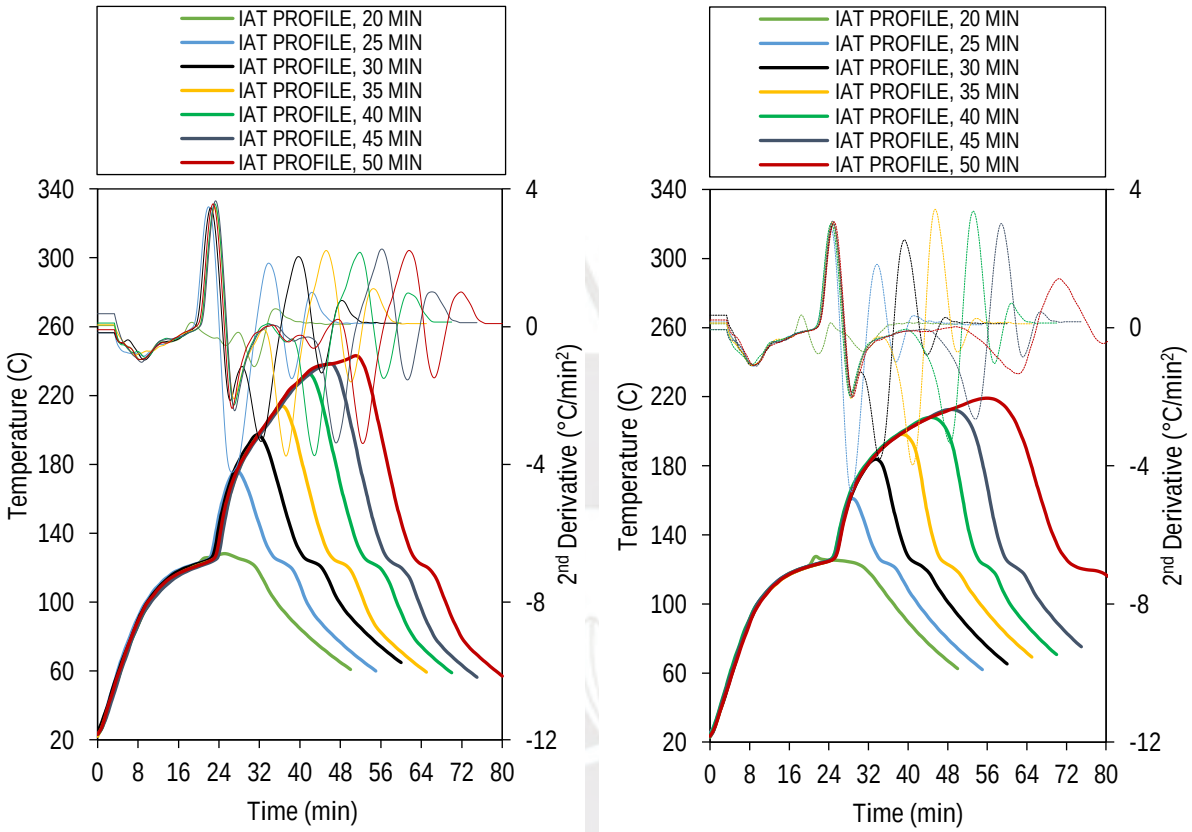

(a) Group A (0% *CWP*). (b) Group B (15% *CWP*).

Fig. 5. Set of *IAT* profiles and their 2nd derivatives.

3.5. Results of characterization tests

3.5.1. Differential scanning calorimetry (DSC) and MFI

In a previous publication [21], DSC tests were conducted on the following materials: (i) virgin *HDPE* (BorPureTM MB6562), (ii) *HDPER* powder and (iii) a rotomolded material made of 100% of *HDPER* (T_H of 320 °C and t_H of 25 min). Results showed that the crystallinity of each material is: (i) 77% for virgin HDPE, (ii) 71% for *HDPER* powder and (iii) 65% for rotomolded *HDPER*. Sen et al. [44] indicate that the crystallinity of *PE* decreases significantly when it is subjected to thermo-oxidative conditions. Furthermore, Kazemi [45] states that the crystallinity of recycled plastics tends to be lower than virgin plastics. Thus, these findings suggest that DSC results are consistent.

It can be observed that the crystallinity of virgin *HDPE* decreases as it is consecutively used in two different manufacturing processes. At the beginning, virgin *HDPE* was used to make plastic caps by

injection molding, and its crystallinity is decreased by 6% at the end of this process. Then, the caps were recycled, chopped, and pulverized to obtain *HDPER* powder. Later, this powder was used for making rotomolded samples. Clearly, the crystallinity decreases by 6% more at the end of that process, too. According to Tamboli et al. [46], crosslinking is induced when a thermoplastic is subjected to thermo-oxidative conditions. As the tested materials were exposed to such conditions during the injection and rotational molding processes, crosslinking may be also responsible for the loss of crystallinity.

On the other hand, the melting temperature of each material is: (i) 137 °C for virgin HDPE, (ii) 133 °C for *HDPER* powder and (iii) 135 °C for rotomolded *HDPER*. This shows that melting temperature of *HDPE* does not change much after being recycled and reprocessed once, which agrees with the results reported in other investigations [45]. Likewise, the *MFI* of each material is: (i) 1,58 g/10min for virgin *HDPE*, (ii) 1,81 g/10min for *HDPER* powder and (iii) 1,57 g/10min for rotomolded *HDPER*. There is not a big difference between the *MFI* of these materials.

3.5.2. Morphology

The morphologies of the rotomolded *WPC* from Group B (15% *CWP*) are shown in the Fig. 6. It is well-known that the formation of a pore-free layer from plastic powder is a consequence of sintering and densification. This layer gradually forms on the mold cavity through the successive adhesion of thinner plastic layers [47-48]. In the case of *WPC*, this process develops in a similar way. However, the adhesion between the *CWP* and *HDPER* is not possible due to their incompatibility. Therefore, during the sintering, the *CWP* get entangled or trapped in the three-dimensional network formed by the coalescence of plastic particles. Consequently, the *CWP* cannot move freely and end up well-distributed within the *HDPER* matrix. It is evident that the portion of the *WPC* layer that is farthest from the mold cavity (inner surface of the cylindrical sample) is the last to densify. By taking a look into this surface it is possible to observe the development of particle coalescence (sintering) and the collapse of the three-dimensional network (densification) when *CWP* are incorporated.

In the morphology of the material molded with a t_H of 20 min (Fig. 6(a)), individual *HDPER* particles are observed since they were the last to adhere to the *WPC* layer. Unlike freshly pulverized particles, those have a regular shape and a smooth-rounded surface. Shape change is evident and it is a consequence of temperature as noted by McDaid [36]. However, it is still possible to distinguish the individual particles because they are lightly adhered to each other and to the underlying surface.

Instead, the morphology of the material molded with a t_H of 25 min (Fig. 6(b)) shows plastic necks that formed due to of *HDPER* particle coalescence. In this case, the network of necks traps and restricts the movement of the *CWP*. The fact that the *HDPER* particles and *CWP* have similar sizes seems to be an advantage for that. Then, the morphology of the material molded with a t_H of 30 min (Fig. 6(c)) shows that densification improves as t_H increases because there is a clear growth of the necks at this point. Finally, a significant reduction in porosity is observed in the morphology of the material molded with a t_H of 40 min (Fig. 6(d)).

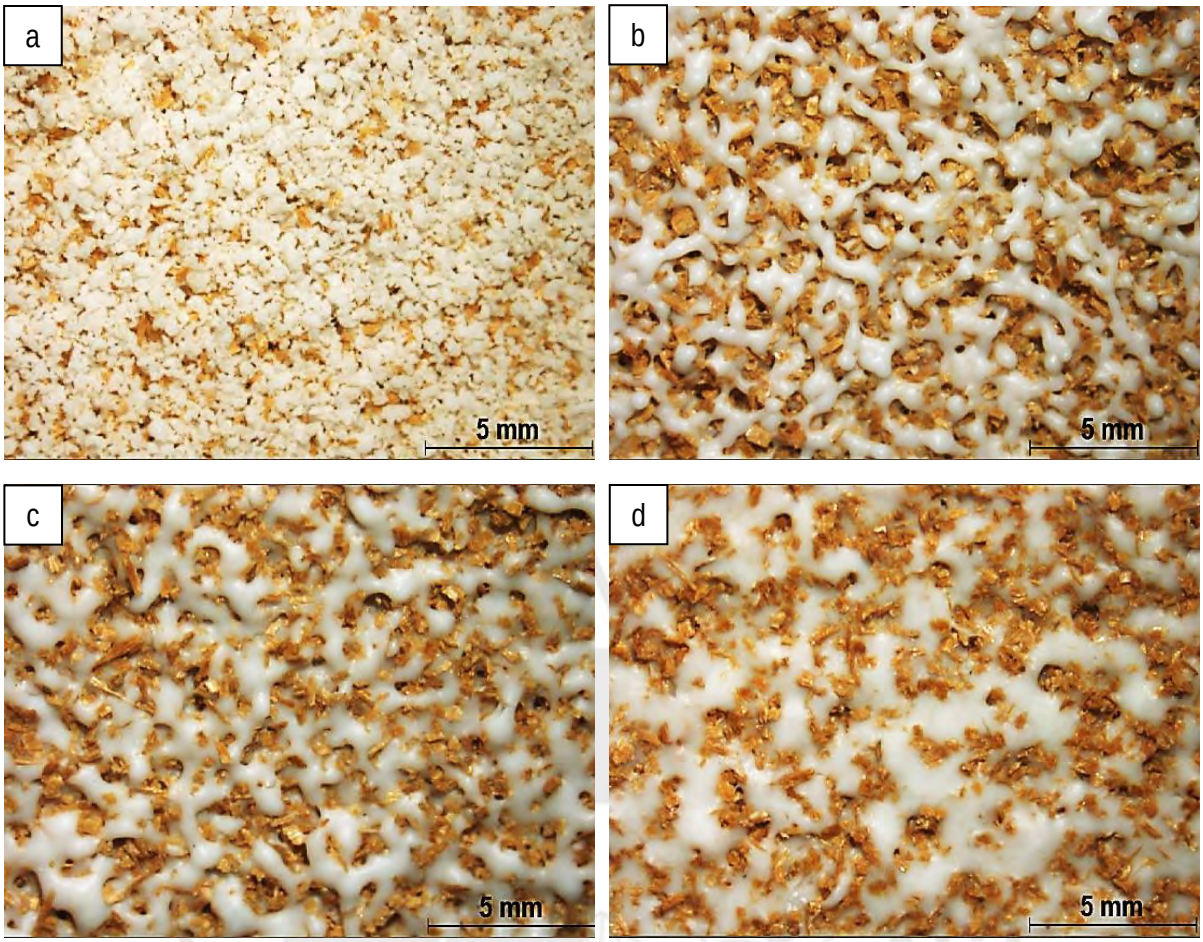

Fig. 6. Morphology of the rotomolded *WPC* from Group B:
(a) 20 min, (b) 25 min, (c) 30 min, (d) 40 min.

The wood-plastic composites made in this research exhibit a remarkable aesthetic appearance since the *CWP* are evenly distributed throughout the entire thickness of the sample. Two things were necessary to achieve this: (i) the use of *CWP* and *HDPER* particles of similar sizes and (ii) the use of a composite powder whose *CWP* are well-distributed due to dry-blending.

3.5.3. Influence of the PIAT on mechanical properties

A. Tensile strength

Fig. 7(a) displays tensile strength of the rotomolded materials from Groups A (0% *CWP*) and B (15% *CWP*). It can be observed that the material molded without *CWP* and a t_H of 40 min (*PIAT* of 233 °C) has a tensile strength of 22 MPa, which is the highest among all. From that point onwards, tensile strength remains constant as it does not increase with the t_H or the *PIAT*. According to this, a rotomolded material made of 100% of *HDPER* is fully densified once the *PIAT* reaches 233 °C. Hence, increasing t_H to achieve a higher *PIAT* is unnecessary as it will not improve tensile strength. An unnecessary extension of t_H may lead to thermal degradation of the material and loss of mechanical properties. It is also important to note that this material reached a PT_{IS} of 230 °C during the heating cycle (see Section 3.4), so this is the highest temperature it was subjected to. It is evident that the material did not undergo thermal degradation since

such process starts at 290 °C for *HDPE* [31, 32]. For a *PIAT* less than 233 °C, tensile strength behavior mainly depends on the level of densification.

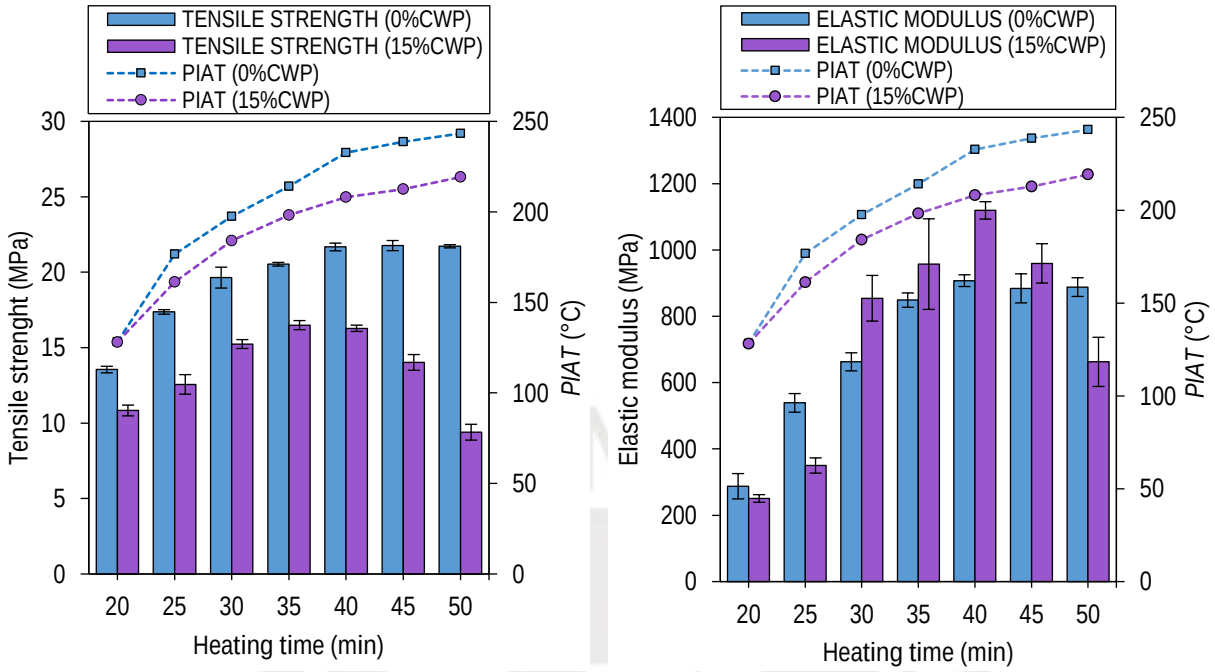

(a) Tensile strength and *PIAT* (b) Elastic modulus and *PIAT*

Fig. 7. Mechanical properties of the rotomolded materials from Groups A and B.

Regarding the materials molded with *CWP*, notice that tensile strength increases from a minimum value of 11 MPa (20 min, *PIAT* of 127 °C) to a maximum value of 16 MPa (40 min, *PIAT* of 208 °C). Afterwards, it decreases to 9 MPa (50 min, *PIAT* of 219 °C). With a *PIAT* lower than 219 °C, it is not possible to achieve thermal degradation of *HDPE* as mentioned above. Therefore, such process is not responsible for the tensile strength behavior in this case. With a *PIAT* < 208 °C, tensile strength behavior is influenced by the level of densification of the composite layer and the presence of *CWP*. As the level of densification improves by increasing the *PIAT*, tensile strength also increases until it reaches a maximum value. With a *PIAT* > 208 °C, results show that the thickness of materials molded with *CWP* increases significantly. This is an indication that those materials become porous once the *PIAT* exceeds that value. It is clear that porosity leads to mechanical weakening, so the tensile strength behavior shown in Fig. 7(a) is strongly associated with this type of defect.

Pores are formed due to the presence of the medium volatile components of capirona wood, which appear during the thermal decomposition of *CWP*. In Section 3.4, it was reported that a material molded with *CWP* reaches a PT_{IS} of 233 °C when the *PIAT* is 208 °C. At this point, initial pore formation is observed. So, it is estimated that medium the volatile components appear when a rotomolded *WPC* is subjected to a PT_{IS} higher than 222°C.

On the other hand, for the same t_H, it is observed that tensile strength of a material molded without *CWP* is higher than tensile strength of material molded with *CWP* for all cases. It is known that adhesion between *HDPER* and *CWP* is poor due to their incompatibility [49], which results in poor load transfer as well [50-51]. Because of this, tensile strength decreases when *CWP* is used. It has been calculated that tensile strength of the material molded with *CWP* is 23% lower than that of the material molded without *CWP* for a t_H of 40 min. These results are consistent with other investigations [17-18, 21, 52-53].

B. Elastic modulus

From the Fig. 7, it is evident that elastic modulus and tensile strength have the same behavior. It also depends on the level of densification or the porosity that arises as a result of the thermal decomposition of *CWP*. Concerning the materials molded without *CWP*, elastic modulus increases from a minimum value of 287 MPa (20 min, *PIAT* of 128 °C) to a maximum value of 907 MPa (40 min, *PIAT* of 233 °C) and, then, it remains constant for higher t_H. Regarding the materials molded with *CWP*, elastic modulus increases from a minimum value of 251 MPa (20 min, *PIAT* of 127 °C) to a maximum value of 1119 MPa (40 min, *PIAT* of 208 °C). Afterwards, it decreases to 663 MPa (50 min, *PIAT* of 219 °C).

Note that, unlike the negative effect of *CWP* on tensile strength, the presence of *CWP* has a positive effect on elastic modulus. In fact, elastic modulus of the material molded with *CWP* increases by 23% compared to the material molded without *CWP*. In this case, both materials were molded with a t_H of 40 min, but they reached a different *PIAT* at the end of the heating cycle. This result is also consistent with the findings reported in other similar studies [17-18, 21, 51-52].

C. Tensile strain

Test results show that tensile strain of materials molded without *CWP* is around 12% and it does not vary significantly with the t_H or the *PIAT*. Similarly, tensile strain of materials molded with *CWP* is 7% when $t_H \leq 35$ min, and it decreases to 4% for a t_H of 50 min. Indeed, tensile strain decreases drastically when *CWP* is used. It has been calculated that tensile strain of the material molded with *CWP* is 45% lower than that of the material molded without *CWP* for a t_H of 40 min. It is clear that the use of *CWP* causes a loss of ductility.

D. Mechanical properties of materials molded with a T_H of 280 °C and 300 °C

The materials from Groups C (T_H of 280 °C) and D (T_H of 300 °C) were also tensile tested. Results show that their mechanical behavior is identical to that of the materials molded with a T_H of 260 °C. When T_H is 280 °C, a t_H of 32 min is necessary for a rotomolded *WPC* to reach a *PIAT* of 207 °C. Under that condition, this material has a tensile strength, an elastic modulus and a tensile strain of 17 MPa, 1104 MPa and 7%, respectively. in the same way, when T_H is 300 °C, a t_H of 26 min is required to reach the same *PIAT* and the same mechanical properties.

Two important things can be inferred from these results. First, the rotomolded materials have a specific *PIAT* that maximizes their mechanical properties. For the rotomolded materials made of 100% of *HDPER*, the *PIAT* should reach 233 °C to achieve that condition. In the case of rotomolded *WPC*, a *PIAT* of 207

°C is required. At this point, it should be clear that these *PIAT* are independent of the molding parameters, such as the T_H. Second, the t_H required to reach a particular *PIAT* decreases as the T_H increases. So, it can be observed that a T_H of 300 °C is the most convenient option as it requires the shortest t_H.

3.5.4. Influence of the PIAT on physical properties

A. Density and porosity

Fig. 8(a) shows the density (green curve) and the porosity (purple curve) of the rotomolded materials from Group A (0% *CWP*). Tensile strength (red curve) and actual thickness (blue curve) of those materials were also included to explain the influence of porosity on the mechanical properties. Additionally, dashed horizontal lines were drawn as reference: (i) density of the injected *HDPE* (0,955 g/cm³, green line), (ii) porosity of a fully densified material (0%, purple line), (iii) tensile strength of the injected *HDPE* (23 MPa, red line), and (iv) nominal thickness of the rotomolded samples (5 mm, blue line)

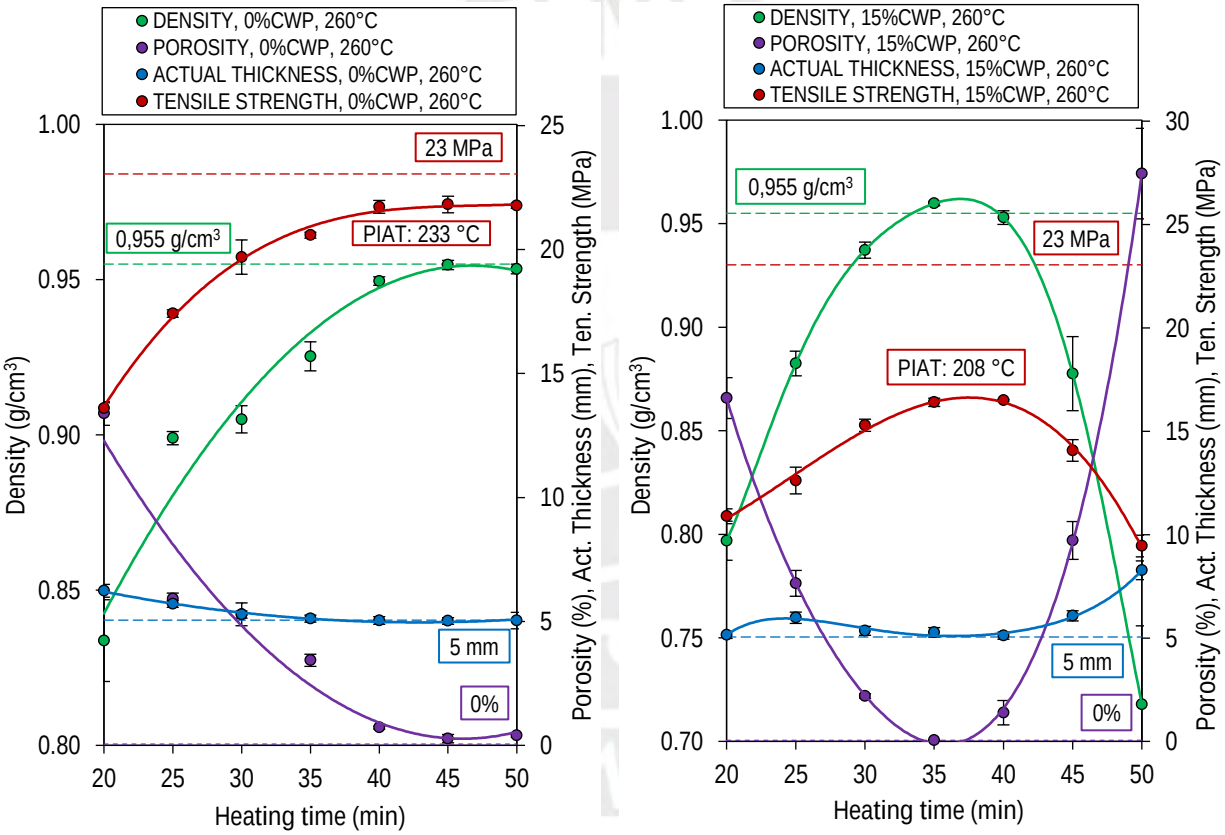

(a) Group A (b) Group B

Fig. 8. Physical properties of the rotomolded materials.

For a material molded without *CWP*, a *PIAT* of 233 °C is required to achieve optimal mechanical properties. Under this condition, it has a density of 0,950 g/cm³ which is practically identical to the density of the injected *HDPE* (0,955 g/cm³). This result indicates that densification has concluded or it is very close to finish. As porosity is minimal at this point (0,7%), mechanical properties are the best. The results regarding the actual thickness also support previous discussions. Clearly, that thickness is equal to the

nominal thickness when the *PIAT* is higher than 233 °C. As pores are eliminating during densification, the thickness of the plastic layer reduces until it reaches the nominal value.

In the case of the materials molded without *CWP* that reached a *PIAT* < 233 °C, it can be affirmed that densification was interrupted since their density is lower than 0,955 g/cm^3. Considering that all of these materials have not fully densified, they have some degree of porosity. This type of defect weakens mechanical performance, as shown in Fig. 8(a). By observing the PT_{IS} values reported in Section 3.4, it can be noticed that thermo-oxidative conditions were not that aggressive to cause thermal degradation of the *HDPER*. Therefore, mechanical behavior basically depends on porosity only.

Similarly, Fig. 8(b) shows the density (green curve) and the porosity (purple curve) of the rotomolded *WPC* from Group B (15% *CWP*). Tensile strength (red curve) and actual thickness (blue curve) of those materials were added. The same dashed horizontal lines of Fig. 8(a)were included as reference, too.

For a material molded with *CWP*, a *PIAT* of 208 °C is required to achieve optimal mechanical properties. In such condition, this material has a density of 0,950 g/cm^3 which is very close to the density of the injected *HDPE* (0,955 g/cm^3). Also, a porosity of 1,3% has been calculated in this case.

In the case of the materials molded with *CWP* that reached a *PIAT* < 208 °C, it can be affirmed that densification was interrupted since their density is lower than 0,955 g/cm^3. As a result, these materials are highly porous because they have not fully densified.

Concerning the materials molded with *CWP* that reached a *PIAT* > 208 °C, it can be stated that densification has concluded. However, all these materials have a density lower than 0,955 g/cm^3, which is not logical. According to the PT_{IS} indicated in Section 3.4, all of these materials were subjected to temperatures above 200 °C. Under these conditions, thermal decomposition of the *CWP* takes place. During this process, the *CWP* release gases (medium volatile components) that cannot flow freely and get trapped within the *WPC* layer. As a consequence, this layer becomes highly porous and looks like a hard sponge. In addition, its density is low because of the high porosity and its actual thickness increases with t_H, as observed in Fig.9. It is evident that the more porous the material, the lower its mechanical properties. For that reason, the decrease of tensile strength is consistent with the increase of porosity.

B. Water absorption

In the case of the materials molded without *CWP*, the water absorption varies from 1,33% (t_H of 20 min) to 0,01% when $t_H \geq 30$ min. The material molded with a t_H of 20 min has high porosity (13%) and, for that reason, water gets trapped within the pores that did not collapse during densification. However, as densification progresses, the water absorption decreases until it reaches the expected value of 0,01%, which is typical of *PE* [54].

In the case of the materials molded with *CWP,* the water absorption varies from 6,87% (t_H of 20 min) to 0,76% (t_H of 50 min). It is clear that the water absorption is notably higher. For example, the material molded with *CWP* that is fully densified (t_H of 40 min, *PIAT* of 208 °C) has a water absorption of 0,56%,

which is the lowest of the materials from Group B. Nevertheless, this is 56 times greater than the water absorption of the material molded without *CWP* that has fully densified.

There are two important aspects to highlight about the water absorption. The materials molded with *CWP* and a *PIAT* lower than 208 °C present incomplete densification and high porosity. In these cases, many *CWP* are prone to absorb water since these are not fully wet by the *HDPER* matrix. For this reason, these materials present high water absorption. On the other hand, the materials molded with *CWP* and a *PIAT* higher than 208 °C have high porosity and low water absorption, which is contradictory. In these cases, the *CWP* are embedded within the *HDPER* matrix, limiting their ability to absorb water. As a result, the water absorption of these materials reaches its minimum value when the *PIAT* exceeds 208 °C.

3.5.5. FTIR

Fig. 10 shows *FTIR* spectra of the rotomolded materials from Group A. In all cases, the four characteristic peaks of *HDPE*: 2914 cm^{-1}, 2848 cm^{-1}, 1463 cm^{-1}, and 718 cm^{-1} are visible [55]. Nevertheless, the spectra of the inner surface of the samples molded with a T_H of 40 min (blue) and 50 min (red) have a particular peak at 1716 cm^{-1}. This peak is located within the region of the carbonyl group (1650 - 1800 cm^{-1}) and its value is related to ketones [56]. The presence of ketones is attributed to low level oxidation of *HDPE* [57-58]. During the heating cycle, the inner surface of these two samples was in contact with the internal air of the mold. So, conditions for the thermo-oxidation of *HDPE* were favorable. As a consequence, these surfaces got a yellowish color at the end of the process. Clearly, thermo-oxidation of *HDPER* begins when an *IAT* higher than 233 °C is reached.

On the other hand, it is interesting to see that the spectrum of the outer surface of the sample molded with a T_H of 50 min (light blue) does not have the peak associated with ketones. In addition, the outer surface did not undergo any color change at the end of the process. The evidences demonstrate that thermo-oxidation did not occur. This result seems contradictory according to the mentioned above, but it is not. As the outer surface is completely adhered to the mold cavity, there is no air in contact with this surface. Consequently, thermo-oxidation of *HDPER* is not possible.

3.5.6. SEM

Fig. 11 shows a *SEM* image of the fracture surface of a tensile test specimen. In this case, the specimen was obtained from a rotomolded *WPC* from Group B that was molded with a T_H of 260°C and t_H of 40 min. According to the previous discussion (see Fig. 8(b)), this material has reached adequate mechanical properties because its porosity is very low, which is also an indication that it has properly densified. Thus, the voids shown in the image are not a consequence of an incomplete densification. Rather, the irregular shape of the voids suggests that a couple of *CWP* were initially there. Since *CWP* were not treated with any type of coupling agent, the *SEM* image proved that there is lack of adhesion between the *CWP* and *HDPER*. As a result, those particles detached from the matrix during the tensile test.

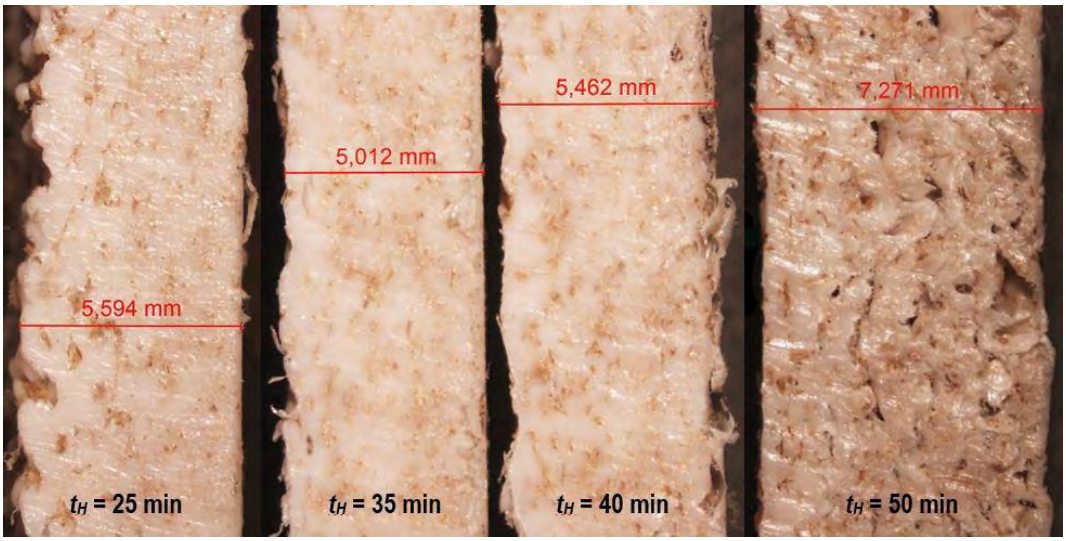

Fig. 9. Actual thickness of the rotomolded materials from Group B.

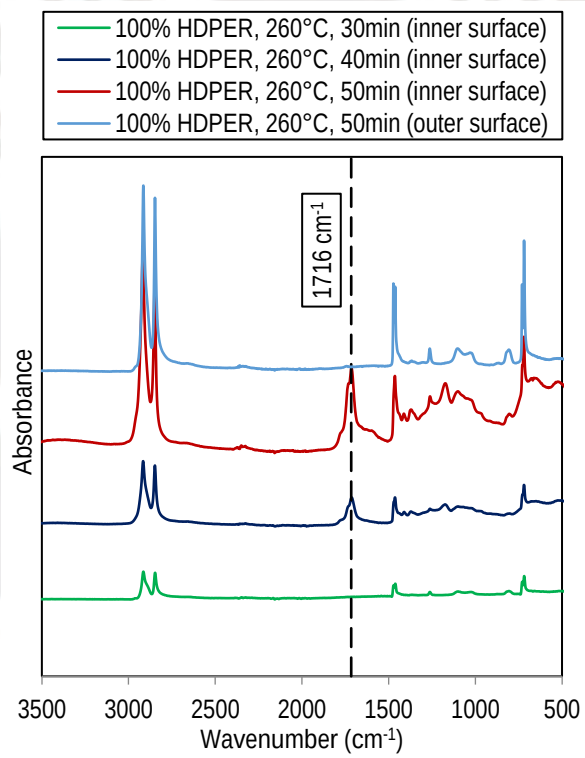

Fig. 10. *FTIR* spectra of the rotomolded materials from Group A.

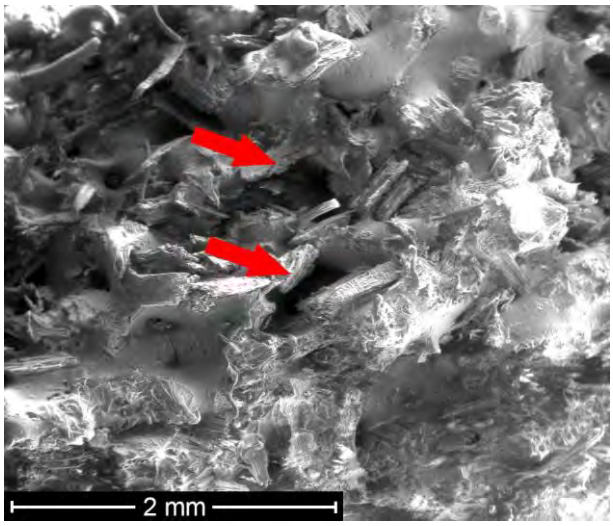

Fig. 11. Facture surface of a tensile test specimen. Rotomolded *WPC* from Group B (t_H of 40 min).

4. CONCLUSIONS

The rotomolded *WPC* show a remarkable aesthetic appearance due to the evenly distribution of the *CWP* throughout the entire thickness of the material. Two things were necessary to achieve this: (i) the use of *CWP* and *HDPER* particles with similar sizes, and (ii) the use of a composite powder where the *CWP* are well-distributed due to the dry-blending.

By using the second derivative of the *IAT* profiles, it was possible to identify the critical points associated with six phases of the rotational molding process. It has been determined that the sintering begins and end when the *IAT* is 91 ± 5 °C and 126 ± 1 °C, respectively. Then, the *IAT* that defines the end of the densification (*PIAT*) depends on the values set for the oven temperature and the heating time. Finally, the crystallization begins and ends when the *IAT* is 133 ± 3 °C and 119 ± 1 °C, respectively.

Results showed that the temperatures associated with the critical points are dependent on the polymer characteristics and are independent of the values set for rotational molding parameters. It also can be affirmed that these temperatures are not affected by the quantity of the *CWP* when this is less than 15%.

It was quantified the negative effect of *CWP* over the sintering. The use of these particles extends the duration of the sintering and hinders plastic particle coalescence. It has been calculated that the duration of the sintering of the material molded with *CWP* is 3 min longer than the material molded without *CWP*.

A relationship between the *PIAT* and the properties of rotomolded materials (mechanical and physical) was presented. Results showed that rotomolded materials are fully densified and reach optimal proprieties when the *PIAT* has a specific value. In the case of the materials with 0% of *CWP*, a *PIAT* of 233 °C is required to achieve such state. For the materials with 15% of CWP a *PIAT* of 208 °C is necessary.

When the *PIAT* ≤ 233 °C, the materials with 0% of *CWP* do not undergo thermal degradation. So, the level of densification, quantified by means of porosity, is responsible for mechanical performance. In the

case of the materials with 15% of *CWP* that happens when the *PIAT* ≤ 208 °C. If the *PIAT* is higher, rotomolded *WPC* become extremely porous because of the medium volatile components of *CWP* that appear as a consequence of the thermal decomposition of the wood. The result of this physical change causes mechanical weakening in the case of rotomolded *WPC*.

In general, the material with 0% of *CWP* that reached a *PIAT* of 233 °C has better properties than the material with 15% of *CWP* that reached a *PIAT* of 208 °C, except for the elastic modulus. Results show that the tensile strength is decreased by 27%, while the elastic modulus is increased by 23%. In addition, tensile strain is decreased by 45% and water absorption is 56 times higher.

It was demonstrated that a plastic powder, obtained from recycled *HDPE* bottle caps made by injection molding, can be used as raw material for the rotational molding process. Using the appropriate molding conditions, the final properties of a rotomolded *HDPER* (consolidated without the application of any external force) can be exactly the same as the injected *HDPER* (consolidated under high pressure). Results show that these properties are independent of the force applied for the material consolidation.

Nomenclature

Notation	Description
WPC	Wood-plastic composites
PE	Polyethylene
HDPER	Recycled high density polyethylene
CWP	Capirona wood particles
T_H	Oven temperature
T_{OS}	Outer surface temperature
T_{IS}	Inner surface temperature
PT_{IS}	Peak inner surface temperature
IAT	Internal air temperature
PIAT	Peak internal air temperature
t_H	Heating time
t_C	Cooling time

Author contributions - (CRediT)

Ademir Vilcayauri-Rios: methodology, investigation, validation, formal analysis, visualization, writing (original draft). Adan Arribasplata-Seguin: conceptualization, methodology, investigation, validation, formal analysis, data curation, writing (review and editing). Roger Quispe-Dominguez: visualization, writing (review and editing). Julio Acosta-Sullcahuamán: conceptualization, funding acquisition, methodology, investigation, project administration, supervision, writing (review and editing). All authors have read and agreed to the published version of the manuscript.

Data availability statement

All data presented in this study is available upon request from the corresponding author. All data is property of PUCP and it is not publicly available. A process of technology transfer is mandatory for any organization that is interested in using data for particular purposes.

Declaration of competing interest

The authors declare no conflict of interest.

Acknowledgments

This research was funded by Fondo Nacional de Desarrollo Científico, Tecnológico y de Innovación Tecnológica (FONDECYT) and Pontifica Universidad Católica del Perú (PUCP), grant number: CONTRATO DE ADJUDICACIÓN DE FONDOS N° 10-2018-FONDECYT/BM – PROGRAMAS DE DOCTORADOS EN ÁREAS ESTRATÉGICAS Y GENERALES.

References

[1] Crawford RJ, Throne JL. Rotational molding technology. Plastics design library. Norwich: William Andrew; 2002.

[2] Crawford, R.J. Recent Advances in the Manufacture of Plastic Products by Rotomolding, Journal of Materials Processing Technology 1996, 56(1-4): 263-271. https://doi.org/10.1016/0924-0136(95)01840-9

[3] León LDVE, Escocio VA, Visconte LLY, Junior JCJ, Pacheco EBAV. Rotomolding and polyethylene composites with rotomolded lignocellulosic materials: a review. J Reinforced Plastics and Composites, 2020; 39(11–12): 459–472. https://doi.org/10.1177/0731684420916529

[4] Torres, F. G., Aguirre, M. Rotational Moulding and Powder Processing of Natural Fibre Reinforced Thermoplastics. International Polymer Processing 2003, 18(2): 204-210. https://doi.org/10.3139/217.1736

[5] Jayaraman, K., Lin, R., Bose, D., Maarouf, M. Natural Fibre-Reinforced Thermoplastics Processed by Rotational Moulding. Advanced Materials Research 2007, (29-30): 307-310. https://doi.org/10.4028/www.scientific.net/AMR.29-30.307

[6] Wang, B., Panigrahi, S., Tabil, L. Crerar, W. Effects of Chemical Treatments on Mechanical and Physical Properties of Flax Fiber-reinforced Rotationally Molded Composites. ASAE/CSAE Annual International Meeting 2004. https://doi.org/10.13031/2013.16956

[7] Wang, B., Panigrahi, S., Tabil, L., Crerar, W. Pre-treatment of Flax Fibers for use in Rotationally Molded Biocomposites. Journal of Reinforced Plastics and Composites 2007, 26(5): 447-463. https://doi.org/10.1177/0731684406072526

[8] Szostak, M., Tomaszewska, N., Kozlowski, R. Mechanical and Thermal Properties of Rotational Molded PE/Flax and PE/Hemp Composites. In: Gapiński, B., Szostak, M., Ivanov, V. Advances in Manufacturing II. Manufacturing. Lecture Notes in Mechanical Engineering, Volume 4, LNME, pp. 495-506, Springer, Cham 2019. https://doi.org/10.1007/978-3-030-16943-5_42

[9] López-Bañuelos, R.H., Moscoso, F.J., Ortega-Gudiño, P., Mendizabal, E., Rodrigue, D., González-Núñez, R. Rotational Molding of Polyethylene Composites Based on Agave Fibers. Polymer Engineering and Science 2012, 52(12): 2489-2497. https://doi.org/10.1002/pen.23168

[10] Cisneros-López, E.O., Pérez-Fonseca, A.A., Fuentes-Talavera, F. J., Anzaldo, J., González-Núñez, R., Rodrigue, D., Robledo-Ortíz, J.R. Rotomolded Polyethylene-Agave Fiber Composites: Effect of Fiber Surface Treatment on the Mechanical Properties. Polymer Engineering and Science 2016, 56(8): 856-865. https://doi.org/10.1002/pen.24314

[11] Cisneros-López, E.O., González-López, M.E., Pérez-Fonseca, A.A., González-Núñez, R., Rodrigue, D., Robledo-Ortíz, J.R. Effect of fiber content and surface treatment on the mechanical properties of natural fiber composites produced by rotomolding. Composite Interfaces 2016, 24(1): 35-53. https://doi.org/10.1080/09276440.2016.1184556

[12] Robledo-Ortíz, J.R., González-López, M.E., Rodrigue, D., Gutiérrez-Ruiz, J.F., Prezas-Lara, F., Pérez-Fonseca, A.A. Improving the Compatibility and Mechanical Properties of Natural Fibers/Green Polyethylene Biocomposites Produced by Rotational Molding. Journal of Polymers and the Environment 2020, 28(3): 1040-1049. https://doi.org/10.1007/s10924-020-01667-1

[13] Abhilash, S.S., Singaravelu, D.L. Effect of Fiber Content on Mechanical and Morphological Properties of Bamboo Fiber-Reinforced Linear Low-Density Polyethylene Processed by Rotational Molding. Transactions of the Indian Institute of Metals 2020 73, 1549-1554. https://doi.org/10.1007/s12666-020-01922-y

[14] Hejna, A., Barczewski, M., Andrzejewski, J., Kosmela, P., Piasecki, A., Szostak, M., Kuang, T. Rotational Molding of Linear Low-Density Polyethylene Composites Filled with Wheat Bran. Polymers 2020, 12(5): 1004. https://doi.org/10.3390/polym12051004

[15] Andrzejewski, J., Krawczak, A., Wesoły, K., Szostak, M. Rotational Molding of Biocomposites with Addition of Buckwheat Husk Filler. Structure-Property Correlation Assessment for Materials Based on Polyethylene (PE) and Poly(Lactic Acid) PLA. Composites Part B: Engineering 2020, (202): Paper 108410. https://doi.org/10.1016/j.compositesb.2020.108410

[16] Gupta, N., Ramkumar, P. Experimental Investigation of Linear Low Density Polyethylene Composites Based on Coir For Rotational Molding Process. Polymers and Polymer Composites 2020, 29(8): 1114-1125. https://doi.org/10.1177/0967391120953246

[17] Raymond, A., Rodrigue, D. Foams and Wood Composite Foams Produced by Rotomolding. Cellular Polymers 2013, 32(4): 199-212. https://doi.org/10.1177/026248931303200401

[18] Hanana, F.E., Rodrigue, D. Rotational Molding of Self-Hybrid Composites Based on Linear Low-Density Polyethylene and Maple Fibers. Polymer Composites 2017, 39(11): 4094-4103. https://doi.org/10.1002/pc.24473

[19] Hanana, F. E., Chimeni, D. Y., Rodrigue, D. Morphology and Mechanical Properties of Maple Reinforced LLDPE Produced by Rotational Moulding: Effect of Fibre Content and Surface Treatment. Polymers and Polymer Composites 2018, 26(4): 299-308. https://doi.org/10.1177/096739111802600404

[20] Hanana, F. E., Rodrigue, D. Effect of Particle Size, Fiber Content, and Surface Treatment on the Mechanical Properties of Maple-Reinforced LLDPE Produced By Rotational Molding. Polymers and Polymer Composites 2020, (29)5: 343-353. https://doi.org/10.1177/0967391120916602

[21] Arribasplata-Seguin, A., Quispe-Dominguez, R., Tupia-Anticona, W., Acosta-Sullcahuamán, J. Rotational molding parameters of wood-plastic composite materials made of recycled high density polyethylene and wood particles. Composites Part B: Engineering 2021, (217): Paper 108876. https://doi.org/10.1016/j.compositesb.2021.108876

[22] Martins, C.I., Gil, V., Rocha, S. Thermal, Mechanical, Morphological and Aesthetical Properties of Rotational Molding PE/Pine Wood Sawdust Composites. Polymers 2022, 14 (1): 193. https://doi.org/10.3390/polym14010193

[23] Nicole, M. Stark, N.M., Cai, Z., Carll, C. Chapter 11: Wood-Based Composite Materials: Panel Products, Glued-Laminated Timber, Structural Composite Lumber, and Wood-Nonwood Composite Materials. In: Ross, R.J. Wood Handbook: Wood as an Engineering Material (Centennial Edition), USDA Forest Service, Forest Products Laboratory 2010.

[24] Klyosov, A.A. Wood-Plastic Composites, John Wiley & Sons, Inc. 2007.

[25] Sliwa, F., El Bounia, N., Marin, G., Charrier, F., Malet, F. A New Generation of Wood Polymer Composite with Improved Thermal Stability. Polymer Degradation and Stability 2012, 97(4): 496-503. https://doi.org/10.1016/j.polymdegradstab.2012.01.023.

[26] Salit, M.S. Chapter 4: Mechanical and Other Related Properties of Tropical Natural Fibre Composites. In: Tropical Natural Fibre: Composites Properties, Manufacture and Applications, Springer Science - Business Media Singapore 2014

[27] Ichazo, M., Albano, C., González, J., Perera, R., Candal, M. Polypropylene/Wood Flour Composites: Treatments and Properties. Composite Structures 2001, 54(2-3): 207-214. https://doi.org/10.1016/S0263-8223(01)00089-7

[28] Cui, Y., Lee, S., Noruziaan, B., Cheung, M., Tao, J. Fabrication and Interfacial Modification of Wood/Recycled Plastic Composite Materials. Composites Part A: Applied Science and Manufacturing 2008, 39(4): 655-661. https://doi.org/10.1016/j.compositesa.2007.10.017

[29] Dou, Y., Rodrigue, D. Rotational molding of hybrid composites based on linear low-density polyethylene/ground tire rubber/maple wood fibers. In: Annual technical conference - ANTEC, conference proceedings, 2018-May; 2018.

[30] Nugent, P. Chapter 06: Rotational Molding. In: Harper, C.A. Handbook of Plastic Processes, John Wiley & Sons, Inc. 2006. https://doi.org/10.1002/0471786586.ch6

[31] Breen, C., Last, P.M., Taylor, S., Komadel, P. Synergic chemical analysis — the coupling of TG with FTIR, MS and GC-MS 2. Catalytic transformation of the gases evolved during the thermal decomposition of HDPE using acid-activated clays. Thermochimica Acta 2000, 363(1-2): 93-104. https://doi.org/10.1016/S0040-6031(00)00599-2

[32] Apone, S., Bongiovanni, R., Braglia, M., Scalia, D., Priola, A. Effects of thermomechanical treatments on HDPE used for TLC ducts. Polymer Testing 2003, 22(3): 275-280. https://doi.org/10.1016/S0142-9418(02)00099-5

[33] Clemons, C.M. Chapter 15: Wood Flour. In: Xanthos, M. Functional Fillers for Plastics. Wiley-VCH Verlag GmbH & Co., 2010. https://doi.org/10.1002/9783527629848

[34] Ward-Perron N, Rodrigue D. Analysis of wood particle drying for rotomolding application. In: Annual Technical Conference - ANTEC, Conference Proceedings, 3; 2012. p. 2259–62.

[35] Throne, J.L., Sohn, M.S. Characterization of Rotational Molding Grade Polyethylene Powders. Advances in Polymer Technology 1989, 9(3): 181-192. https://doi.org/10.1002/adv.1989.060090302

[36] McDaid, J.M. The grinding of polyethylene powders for use in rotational moulding, Ph.D. Thesis in Mechanical and Manufacturing Engineering, The Queen's University of Belfast 1998.

[37] González-Núñez, R., Moscoso-Sánchez, F.J., Aguilar, J., López-GonzálezNúñez, R.G., Robledo-Ortíz, J.R., Rodrigue, D. Thermal analysis of foamed polyethylene rotational molding followed by internal air temperature profiles. Polymer Engineering & Science 2017, 58(S1): E235-E241. https://doi.org/10.1002/pen.24725

[38] Kontopoulou, M., Vlachopoulos, J. Bubble Dissolution in Molten Polymers and Its Role in Rotational Molding, Polymer Engineering and Science 1999, 39(7): 1189-1198. https://doi.org/10.1002/pen.11505

[39] Gogos, G. Bubble Removal in Rotational Molding, Polymer Engineering and Science 2004, 44(2): 388-394. https://doi.org/10.1002/pen.20035

[40] Torres, F.G., Aguirre, M. Rotational Moulding and Powder Processing of Natural Fibre Reinforced Thermoplastics. International Polymer Processing 2003, 18(2): 204-210. https://doi.org/10.3139/217.1736

[41] Bergman, T.L., Lavine, A.S., Incropera, F.P., Dewitt, D.P., Introduction to Heat Transfer Sixth Edition (Solution Manual). John Wiley & Sons, Inc. 2011.

[42] Yang, C., Navarro, M.E., Zhao, B., Leng, G., Xu, G., Wang, L., Ding, Y. Thermal conductivity enhancement of recycled high density polyethylene as a storage media for latent heat thermal energy storage. Solar Energy Materials and Solar Cells 2016, 152: 103-110. https://doi.org/10.1016/j.solmat.2016.02.022

[43] Zepeda-Rodríguez, Z., Arellano-Martínez, M.R., Cruz-Barba, E., Zamudio-Ojeda, A., Rodrigue, D., Vázquez-Lepe, M., González-Núñez, R. Mechanical and thermal properties of polyethylene/carbon nanofiber composites produced by rotational molding. Polymer Composites 2019, 41(4): 1224-1233. https://doi.org/10.1002/pc.25448

[44] Sen, A.K., Kumar, R. Study of the change of crystallinity of polyethylene on oxidation by inverse phase gas chromatography. Journal of Applied Polymer Science 1988, 36(1): 205-213. https://doi.org/10.1002/app.1988.070360116

[45] Kazemi Najafi S. Use of recycled plastics in wood plastic composites - a review. Waste Manag 2013;33(9):1898–905. https://doi.org/10.1016/j.wasman.2013.05.017

[46] Tamboli, S.M., Mhaske, S.T., Kale, D.D. Crosslinked polyethylene. Indian Journal of Chemical Technology 2004, 11(6): 853-864.

[47] Löhner, M., Drummer, D. Characterization of Layer Built-Up and Inter-Layer Boundaries in Rotational Molding of Multi-Material Parts in Dependency of the Filling Strategy, Journal of Polymer Engineering 2017, 37(4): 411-420. https://doi.org/10.1515/polyeng-2016-0175

[48] Torres, F.G. Chapter 8: Rotational moulding of polymers. In: Thomas, S., Weimin, Y. Advances in polymer processing, Woodhead Publishing Limited 2009.

[49] Saheb, D.N., Jog, J.P. Natural fiber polymer composites: A review. Advances in Polymer Technology 1999, 18(4): 351-363. https://doi.org/10.1002/(SICI)1098-2329(199924)18:4<351::AID-ADV6>3.0.CO;2-X

[50] Al-Maadeed, M.A., Labidi, S. Chapter 4: Recycled Polymers in Natural Fibre-Reinforced Polymer Composites. In: Hodzic, A., Shanks, R. Natural Fibre Composites – Materials, Processes and Properties, Woodhead Publishing Limited 2014.

[51] Bledzki, A. K., Reihmane, S., Gassan, J. Thermoplastics Reinforced with Wood Fillers: A Literature Review. Polymer-Plastics Technology and Engineering 1998, 37(4): 451-468. http://dx.doi.org/10.1080/03602559808001373

[52] Ward-Perron, N., Rodrigue, D., Natural Fiber Reinforced Thermoplastics (NFRTP) Processed By Rotomolding, SPE/ANTEC (2012).

[53] Raymond, A., Rodrigue, D. Wood Plastics Composites Produced by Rotomolding, SPE ANTEC (2013).

[54] Harper, C.A. Modern Plastics Handbook, McGraw-Hill Companies, Inc. 2000.

[55] Gulmine, J., Janissek, P., Heise, H., Akcelrud, L. Polyethylene characterization by FTIR. Polymer Testing 2002, 21(5): 557–563. https://doi.org/10.1016/S0142-9418(01)00124-6

[56] Cuadri, A.A., Martín-Alfonso, J.E. The effect of thermal and thermo-oxidative degradation conditions on rheological, chemical and thermal properties of HDPE. Polymer Degradation and Stability 2017, 141: 11–18. https://doi.org/10.1016/j.polymdegradstab.2017.05.005

[57] Singh, B., Sharma, N. Mechanistic implications of plastic degradation. Polymer Degradation and Stability 2008, 93(3): 561-584. https://doi.org/10.1016/j.polymdegradstab.2007.11.008

[58] Corrales, T., Catalina, F., Peinado, C., Allen, N.S., Fontan, E. Photooxidative and thermal degradation of polyethylenes: interrelationship by chemiluminescence, thermal gravimetric analysis and FTIR data. Journal of Photochemistry and Photobiology A: Chemistry 2002, 147(3): 213-224. https://doi.org/10.1016/S1010-6030(01)00629-3